ENERGY DEPENDENCE OF PION PRODUCTION BY PROTONS ON NUCLEI

P.H. Pile, R.D. Bent, R.E. Pollock, P.T. Debevec,* R.E. Marrs,** and M.C. Green

The reactions $^{10}B(p,\pi^+)^{11}B(g.s.)$ and $^{40}Ca(p,\pi^+)$ $^{41}Ca(g.s.)$ have been studied with proton beams in the energy range 140 to 200 MeV. Angular distributions at several energies, supplemented with fixed angle cross section data at several other energies, establish for the first time the energy dependence of these reactions in the near-threshold region.

The differential cross sections were measured with two different magnetic spectrometers. The larger quadrupole-dipole-dipole-multipole (QDDM) instrument,[1] used for the pion energy region above 9 MeV, is in routine use for precise proton elastic scattering studies, which confirm the solid angle and beam charge collection, giving total systematic uncertainties in the range 5% to 15% for the absolute cross sections in the present pion measurements. The smaller instrument, used for pion energies below 13 MeV, consists of two opposing dipoles ($D\bar{D}$). It has a 3.5 msr solid angle, 77 cm flight path, and a mixed scintillator and silicon detector telescope at the non-dispersed focal point. The $D\bar{D}$ was developed especially for (p,π^+) measurements and is described in detail elsewhere.[2] Systematic errors in the absolute cross sections measured with this instrument are believed to be less than 20 percent. Pions of energies between 9 and 13 MeV can be measured with both instruments and the overlapping data are in good agreement. This argues strongly for a correct absolute scale for data from either device.

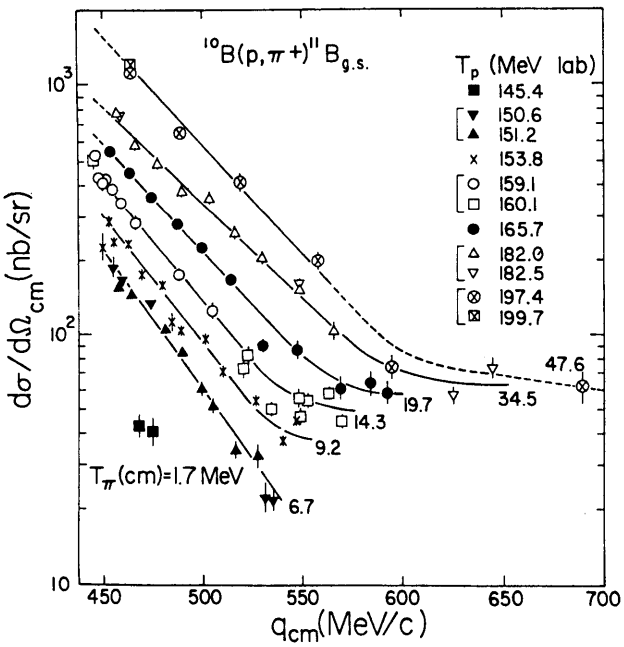

Fig. 1. The $^{10}B(p,\pi^+)^{11}B(g.s.)$ differential cross sections at seven energies plotted as a function of momentum transfer. The curves are guides for the eye.

Differential cross sections for the reaction $^{10}B(p,\pi^+)^{11}B(g.s.)$ at seven proton energies are shown in Fig. 1 plotted against momentum transfer q. The figure shows that to a first approximation the shape is exponential with q below 540 MeV/c, and that while the yield at the smaller angles increases markedly with bombarding energy, the slope of the exponential changes only slightly over this substantial range of energies. Two of the distributions (T_p = 153.8 and 160.1 MeV) extend forward to 0° and offer little experimental evidence for a forward minimum due to the $|\vec{k}_\pi - \lambda \frac{m_\pi}{m_p} \vec{k}_p|^2$ factor, which comes from the non-relativistic reduction of the pion production operator and appears as a multiplicative factor in the expression for the differential cross section given by the one-nucleon-model (ONM) in the plane-wave approximation.

The energy dependence of the exponential portion of the Boron angular distributions can be parameterized by a normalization factor (differential cross section at fixed q) and a slope factor. For a fixed forward angle the reaction kinematics shows q changing only slowly with beam energy, so that the differential cross section data at fixed laboratory angle is representative of the energy variation of this normalization factor.

Figure 3a shows twelve θ_π(lab) = 25° measurements of the $^{10}B(p,\pi^+)^{11}B$(g.s.) cross section plotted against the pion center-of-mass momentum η_π (in units of $m_\pi c$). The range of pion energies in the center of mass extends from 1.7 to 47.6 MeV. Points from Uppsala[3] and Orsay[4] are shown for comparison. Although the cross sections measured with the DD̄ and QDDM spectrographs using quite different detectors agree well within the systematic measurement errors at η_π(cm) = 0.37, they are larger than those measured at Uppsala[3] and Orsay[4] by factors of about 1.7 and 5, respectively.

To illustrate the importance of Coulomb and angular momentum barriers in determining the energy dependence for this target, Fig. 3a shows a curve generated from the exterior Coulomb penetrability $P_\ell(\eta) = \eta_\pi / (F_\ell^2 + G_\ell^2)$ evaluated at $R = 1.25A^{1/3}$fm. The curve is a linear combination of the form $AP_0 + B\sqrt{P_0P_1} + CP_1$ where the constants, A, B and C are determined

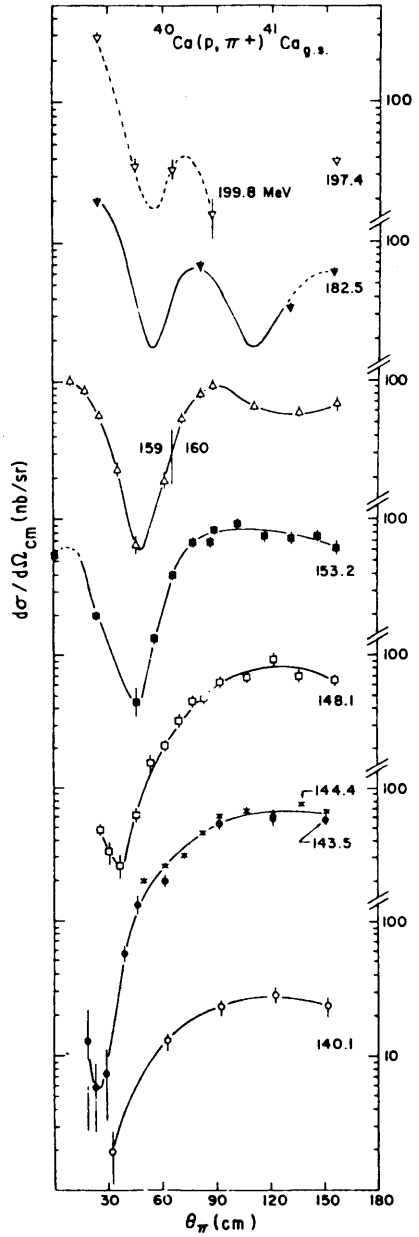

Fig. 2. The $^{40}Ca(p,\pi^+)^{41}Ca$(g.s.) differential cross sections at seven energies. Note the motion of the minimum toward forward angles as the energy approaches threshold and the near-constancy of the 90° yield except at the lowest and highest energies. The curves are guides for the eye.

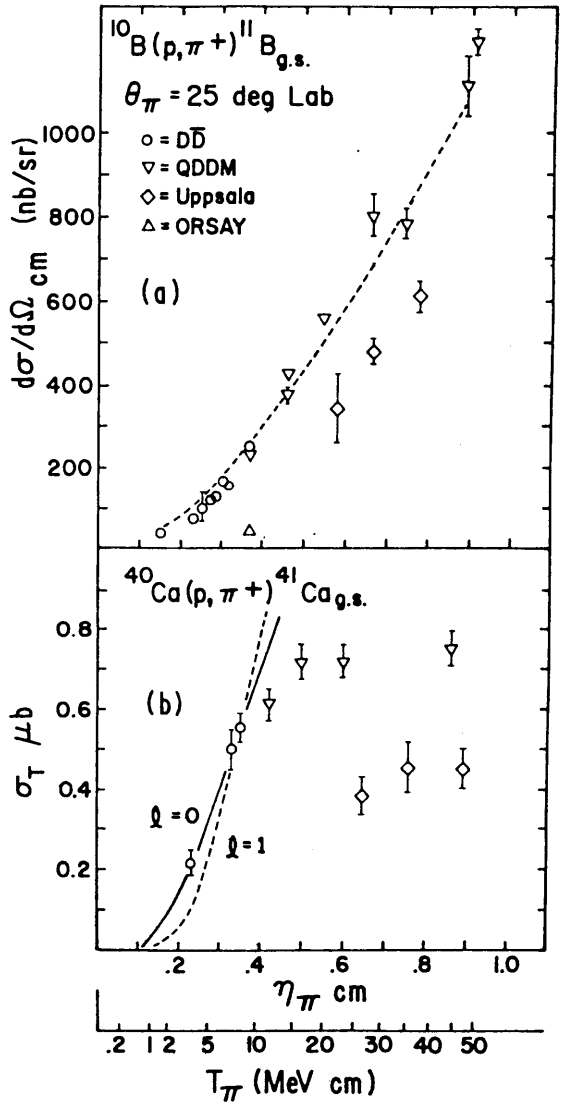

Fig. 3(a). The dependence of the $^{10}B(p,\pi^+)^{11}B_{g.s.}$ differential cross section at θ_π(lab) = 25° on pion center-of-mass momentum (in units of $m_\pi c$). Where not shown, the error bars are smaller than the data points. (b). The dependence of the $^{40}Ca(p,\pi^+)^{41}Ca_{g.s.}$ total cross section on pion center-of-mass momentum. The curves are explained in the text.

primarily by the shape of the angular distribution at one pion energy ($\sim$ 15 MeV) chosen such that only s and p wave pions can be emitted with appreciable probability, and P_0 and P_1 are the s and p wave penetrabilities respectively. The reasonably close correspondence between this curve and the data in Fig. 3a indicates that the energy dependence is dominated by barrier factors for this nucleus over an appreciable energy range.

Differential cross sections for the reaction $^{40}Ca(p,\pi^+)^{41}Ca(g.s.)$ at seven bombarding energies are shown in Fig. 2. Smooth curves have been drawn through the data points to guide the eye. The 182.5 MeV curve is the Uppsala[3,5] 185 MeV angular distribution normalized to our four data points. The Orsay 154 MeV data[6] (muliplied by a factor of 2.2 to normalize to our θ_π (lab) = 25° point) were used to determine the shape of the 153 MeV curve at forward angles.

The $^{40}Ca(p,\pi^+)^{41}Ca(g.s.)$ angular distribution exhibit a well-defined and systematic variation in shape with changing bombarding energy which is in sharp contrast to the behavior of the $^{10}B(p,\pi^+)^{11}B(g.s.)$ reaction. The deep minimum seen near 60° at 185 MeV bombarding energy[5] becomes deeper (ratio $\sigma_{90°}/\sigma_{min}$ approaches 100:1 at T_π = 7.6 MeV) and moves toward forward angles as the energy is lowered toward threshold. The yield at 90° stays nearly constant until T_π (cm) is below 10 MeV. The momentum transfer q at the forward minimum varies linearly with p_π according to $dq/dp_\pi = 0.82 \pm 0.09$ over a range including the 148, 153, and 160 MeV energies shown here and the three higher energies quoted in Ref. 3. The energy dependence of the depth and position of the first minimum was not reproduced in the DWBA one-nucleon mechanism calculations of Höistad.[3] Similar calculations have been made by Tsangarides et al.,[7] who investigated the sensitivity of the model to different pion-nucleus optical potentials. Although they found it was possible to reproduce the behavior of the first minimum in the $^{40}Ca(p,\pi^+)$ angular distributions by using a modified Laplacian pion-nucleus potential with damping of off-shell effects, the calculated cross sections were too large by about a factor of two, the second minimum in the Uppsala 185 MeV angular distribution[5] was not reproduced and fits to the pion-elastic scattering data were poor, especially at large angles. It is well known that calculations of this type are extremely sensitive to details of the pion-nucleus optical potentials.

The motion of the minimum in these data can confuse the interpretation[8,9] of the energy dependence of forward angle cross sections for this nucleus. The total cross sections obtained by integration of the differential cross sections are shown plotted against pion momentum in Fig. 3b. The Uppsala[3] measurements are shown for comparison. For this case, in contrast with Fig. 3a, Coulomb penetrability arguments can explain the energy variation only for the lowest energy points. There is strong suppression of yield at pion energies greater than 10 MeV. The Coulomb penetrability functions plotted in this figure are evaluated at $R = 1.25A^{1/3}$ fm as in Fig. 3a but show the ℓ=0 and ℓ=1 components separately (normalized to the data at $\eta_\pi = 0.35$). The energy-dependent behavior of the second minimum which has begun to develop at 185 MeV, and which may be a true minimum in the form-factor of the bound neutron, is of particular interest for future investigation.

*Department of Physics, University of Illinois, Urbana, Illinois 61801.

**TRIUMF, University of British Columbia, Vancouver 8, British Columbia, Canada.

1) R.D. Bent, P.T. Debevec, P.H. Pile, R.E. Pollock, R.E. Marrs, and M.C. Green, Phys. Rev. Letters 40, 495 (1978).

2) P.H. Pile, Ph.D. Thesis, Indiana University, 1978 (unpublished) and Bull. Am. Phys. Soc. 23, 611 (1978).

3) B. Höistad, High Energy Physics and Nuclear Structure Conference Proceedings, Zürich, Switzerland, edited by M.P. Locher, 215 (1977).

4) Y. Le Bornec, B. Tatischeff, L. Bimbot, I. Brissaud, J.P. Garron, H.D. Holmgren, F. Reide, and N. Willis, Phys. Letters 49B, 434 (1974).

5) S. Dahlgren, P. Grafström, B. Höistad, and A. Åsberg, Nucl. Phys. A227, 245 (1974).

6) Y. Le Bornec, G. Tatischeff, L. Bimbot, I. Brissaud, H.D. Holmgren, J. Källne, F. Reide, and N. Willis, Phys. Letters 61B, 47 (1976).

7) M. Tsangarides, J.G. Wills, and R.D. Bent, Bull. Am. Phys. Soc. 23, 952 (1978).

8) J.V. Noble, Phys. Rev. Letters 37, 123 (1976).

9) L.D. Miller and H.J. Weber, Phys. Rev. C 17, 219 (1978).